

# Detection and Characterization of Cellular Immune Responses Using Peptide–MHC Microarrays

Yoav Soen<sup>1</sup>, Daniel S. Chen<sup>2,5</sup>, Daniel L. Kraft<sup>3</sup>, Mark M. Davis<sup>4,5\*</sup>, Patrick O. Brown<sup>1,5\*</sup>

**1** Department of Biochemistry, Stanford University, Stanford, California, United States of America, **2** Department of Internal Medicine, Division of Oncology, Stanford University, Stanford, California, United States of America, **3** Department of Pediatrics, Division of Bone Marrow Transplant, Stanford University, Stanford, California, United States of America, **4** Department of Microbiology and Immunology, Stanford University, Stanford, California, United States of America, **5** Howard Hughes Medical Institute, Stanford University, Stanford, California, United States of America

**The detection and characterization of antigen-specific T cell populations is critical for understanding the development and physiology of the immune system and its responses in health and disease. We have developed and tested a method that uses arrays of peptide–MHC complexes for the rapid identification, isolation, activation, and characterization of multiple antigen-specific populations of T cells. CD4<sup>+</sup> or CD8<sup>+</sup> lymphocytes can be captured in accordance with their ligand specificity using an array of peptide–MHC complexes printed on a film-coated glass surface. We have characterized the specificity and sensitivity of a peptide–MHC array using labeled lymphocytes from T cell receptor transgenic mice. In addition, we were able to use the array to detect a rare population of antigen-specific T cells following vaccination of a normal mouse. This approach should be useful for epitope discovery, as well as for characterization and analysis of multiple epitope-specific T cell populations during immune responses associated with viral and bacterial infection, cancer, autoimmunity, and vaccination.**

## Introduction

Antigen-specific cellular immune responses are mediated by a diverse population of T cells, each capable of recognizing a specific peptide bound to a particular major histocompatibility complex (MHC) molecule on the surface of host cells. Recognition of peptides bound to class I or class II MHC molecules leads to the clonal expansion, activation, and maturation of T lymphocytes, resulting in effector populations of either cytotoxic (CD8<sup>+</sup> CTL) or helper (CD4<sup>+</sup>) T cells, respectively. The presence of antigen-specific effector cells is diagnostic of an immune response specific to that antigen; detection of these antigen-specific cells is therefore critical for the characterization of the response and for understanding its natural course. In addition, a systematic survey of the global repertoire of T cell specificities, its dynamics over time and between individuals, could be of great value in elucidating the inner workings of the immune system and for designing efficient strategies for immunization, immunotherapy, and treatment of autoimmune disease.

The development of peptide–MHC tetramers (Altman et al. 1996) and dimers (Greten et al. 1998) has allowed visualization of antigen-specific T cells by flow cytometry and, more recently, in situ (Haanen et al. 2000) approaches. This has led to characterization of T cell responses to specific antigens associated with microbial pathogens (Callan et al. 1998; Ogg et al. 1998a; Smith et al. 2000), autoimmunity (Ogg et al. 1998b), allergens (Seneviratne et al. 2002), and cancer cells (Lee et al. 1999; Mollred et al. 2000). Unfortunately, while a significant improvement over previous approaches, the use of multimeric soluble peptide–MHC constructs in flow cytometry is technically difficult, time consuming, expensive, and, most importantly, limited to only one or a very few antigen specificities at a time. cDNA-based expression libraries and various forms of combinatorial synthetic peptide libraries,

such as the positional scanning combinatorial library (Pinilla et al., 1994; Ignatowicz et al. 1996) and bead-bound libraries (Hiemstra et al. 1997, 1998a, 1998b), have also been utilized in attempts to study T cell receptor (TCR) specificity and reactivity. However, these approaches have been hampered by the intrinsic limitations of indirect readouts, such as proliferation assays, and by the complexity of the libraries, which do not allow for the direct visualization of T cell interactions with diverse, but individually distinguishable, antigens presented by an MHC complex. Consequently, the various peptide library approaches are mainly effective when used in combination with relatively homogeneous T cell populations, such as T cell clones.

Here we report the development of a cellular array-based screening strategy using microarrays of immobilized peptide–MHC complexes. This approach is very rapid and allows the simultaneous identification, isolation, characterization, and

Received August 21, 2003; Accepted October 5, 2003; Published December 22, 2003

DOI: 10.1371/journal.pbio.0000065

Copyright: ©2003 Soen et al. This is an open-access article distributed under the terms of the Creative Commons Attribution License, which permits unrestricted use, distribution, and reproduction in any medium, provided the original work is properly cited.

Abbreviations: BSP, BirA substrate peptide; CTL, cytotoxic T lymphocyte; DIC, differential interference contrast; FACS, fluorescence-activated cell sorting; FCS, fetal calf serum; FITC, fluorescein isothiocyanate; HLA, human leucocyte antigen; LCMV, lymphocytic choriomeningitis virus; mAb, monoclonal antibody; MCC, moth cytochrome C; MHC, major histocompatibility complex; OVA, ovalbumin; PBS, phosphate-buffered saline; PE, phycoerythrin; SA, streptavidin; TCR, T cell receptor; TRP, tyrosinase-related protein

Academic Editor: Philippa Marrack, National Jewish Medical and Research Center

\*To whom correspondence should be addressed. E-mail: mdavis@pmgm2.stanford.edu (MMD), pbrown@cmgm.stanford.edu (POB)

These authors contributed equally to this work.



activation of multiple antigen-specific populations of T cells. Antigen-specific cells are captured onto an array of individual spots of peptide–MHC complexes, with cell capture at each spot being dependent on T cell specificity. We investigated the specificity of binding and the limit of detection achievable by this method, using differentially labeled CD8<sup>+</sup> and CD4<sup>+</sup> T cells of defined specificity from transgenic mice. We also found that T cell activation, upon binding to the appropriate peptide–MHC on the array, could be detected by visualizing a transient increase in intracellular calcium. Finally, we have applied this method to detect a weak, specific immune response in a normal mouse following subcutaneous vaccination with ovalbumin (OVA). The sensitivity and specificity of this approach, together with the ability to survey a large number of specificities quickly and easily, may provide a practical way to detect and screen for natural immune responses and to characterize variations in the T cell repertoire in healthy individuals and in a wide variety of disease states.

## Results

### Construction of a Peptide–MHC Array

Detection of antigen-specific T cells using arrays of peptide–MHC complexes was tested. We prepared phycoerythrin (PE)-labeled peptide–MHC tetramers with the MHC class I (H-2K<sup>b</sup>) murine antigen OVA and MHC class II (I-E<sup>k</sup>) murine antigen moth cytochrome C (MCC), as described (Altman et al. 1996). Both tetramers were validated by fluorescence-activated cell sorting (FACS) analysis using OVA-specific T cells isolated from OT-1 TCR transgenic mice (Hogquist et al. 1994) and MCC-specific 5c.c7 TCR transgenic mice (Fazekas de St. Groth et al. 1993), respectively. To facilitate a comparison between peptide–MHC-mediated and antibody-mediated binding, the OVA and MCC tetramers were arrayed along with antibodies against several mouse lymphocyte cell surface antigens. Hence, individual MHC tetramers and several monoclonal antibodies (mAbs) were prepared in a 384-well plate at various concentrations and dispensed in triplicate onto polyacrylamide film-coated glass slides. The latter were determined to be inert for cell binding while having a high capacity for protein deposition with relatively high fidelity, as compared with a derivatized glass slide (aldehyde-, Poly-L-Lysine-, and nitrocellulose-coated slides were tested).

MHC tetramers and antibodies were arrayed using a piezoelectric noncontact arrayer, which minimizes film disruption and allows control over spot size and the quantity of material deposited, by enabling multiple nanoliter-scale drops to be deposited onto each spot. The resulting spot size with ten 0.45 nl drops (dispensed at a concentration of 1 μg/μl) was approximately 400 μm in diameter. Each spot of this size could accommodate approximately 1,600 closely packed T cells. Suspended cells were subsequently layered onto the array and were allowed to interact with the predispensed tetramers and antibodies (Figure 1A). Following a short period of incubation, the slide was washed to remove unbound cells and visualized by direct inspection, differential interference contrast (DIC), or fluorescence microscopy. Inspection by eye revealed tight, nearly confluent cell clusters on both the antibody and the MHC tetramer spots (Figure 1B).

To optimize the conditions for specific cell capture, we investigated the relationship between the surface density of the peptide–MHC complexes and the number of bound cells (a detailed example is described in Supporting Information; see, as part of this example, Figure S1). For a sufficiently dense tetramer concentration, we found that the binding of OT-1 cells to spots of OVA/K<sup>b</sup> tetramer (OVA peptide 258–265, H-2K<sup>b</sup> class I MHC molecule, β<sub>2</sub>-microglobulin) or 5c.c7 cells to MCC/E<sup>k</sup> tetramer (MCC peptide 88–103, I-E<sup>k</sup> class II MHC molecule, β<sub>2</sub>-microglobulin) was as efficient as the binding to spots of mAbs specific to cell surface markers, and for a sufficiently dense cell suspension, confluent cell binding to the OVA/K<sup>b</sup> tetramer could be achieved with 0.4–0.8 ng of OVA/K<sup>b</sup> tetramer per spot (corresponding to a spotting solution concentration of 0.1–0.2 mg/ml).

### Identification and Isolation of Antigen-Specific Cytotoxic (CD8<sup>+</sup>) and Helper (CD4<sup>+</sup>) T Cells

We tested the specificity of binding to individual spots by using pure populations of differentially labeled, antigen-specific CTLs and helper T cells from transgenic mice. Antigen-specific lymphocytes from OT-1 and 5c.c7 transgenic mice were activated and expanded by adding 1 μM OVA and MCC peptides to the respective single-cell suspensions on day 0, and IL-2 (30 U/ml) was supplemented on day 1. On day 7, active OT-1 (CD8<sup>+</sup>) and 5c.c7 (CD4<sup>+</sup>) lymphocytes were labeled with DiO or DiD-lipophilic tracers, respectively. The two differentially labeled lymphocyte suspensions were mixed in a 1:1 ratio and coincubated on the peptide–MHC array. Following a 10-min incubation at 20°C, the array was washed twice in RPMI medium and examined by fluorescence microscopy (Figure 2). While anti-CD3 and anti-CD28 mAb spots captured both lymphocyte populations, the arrayed MCC/E<sup>k</sup> and OVA/K<sup>b</sup> tetramers exclusively captured the MCC-specific (red) and OVA-specific (green) cells, respectively. The nearly complete segregation of OT-1 and 5c.c7 cells on the appropriate spots illustrates the highly specific nature of lymphocyte capture and the feasibility of array-based T cell sorting and analysis.

### Detection of Antigen-Specific T Cells in Complex Cell Populations Using a Peptide–MHC Array

To directly assess the feasibility of detecting rare T cell specificities in a complex population, we prepared synthetic mixtures of differentially labeled, antigen-specific CTLs and T helper cells, diluted with syngeneic wild-type lymph node cells (Figure 3A) or splenocytes (Figure 3B). DiD-labeled OT-1 cells were diluted 1:100 (Figure 3A, top panels) and 1:1,000 (bottom panels) in DiO-labeled C57BL/6 mouse lymph node cells that had been depleted of monocytes using anti-CD11b beads (to remove cells capable of peptide-independent binding to the MHC complex). OT-1 cells of  $2.7 \times 10^4$  (Figure 3A, top panels) and  $4.41 \times 10^3$  (Figure 3A, bottom panels) were mixed with  $2.7 \times 10^6$  and  $4.41 \times 10^6$  of CD11b-depleted lymph node cells, respectively. The two different mixtures were then separately incubated with identical peptide–MHC arrays, each printed with OVA/K<sup>b</sup> tetramer, LCMV/K<sup>d</sup> control tetramer (lymphocytic choriomeningitis virus gp peptide 33–41, H-2K<sup>d</sup> class I MHC molecule, β<sub>2</sub>-microglobulin), MCC/E<sup>k</sup> tetramer, and three different antibody spots (mouse anti-CD8, mouse anti-CD4, and mouse anti-CD28). Following a 10–30 min incubation at 20°C or 37°C (similar results were

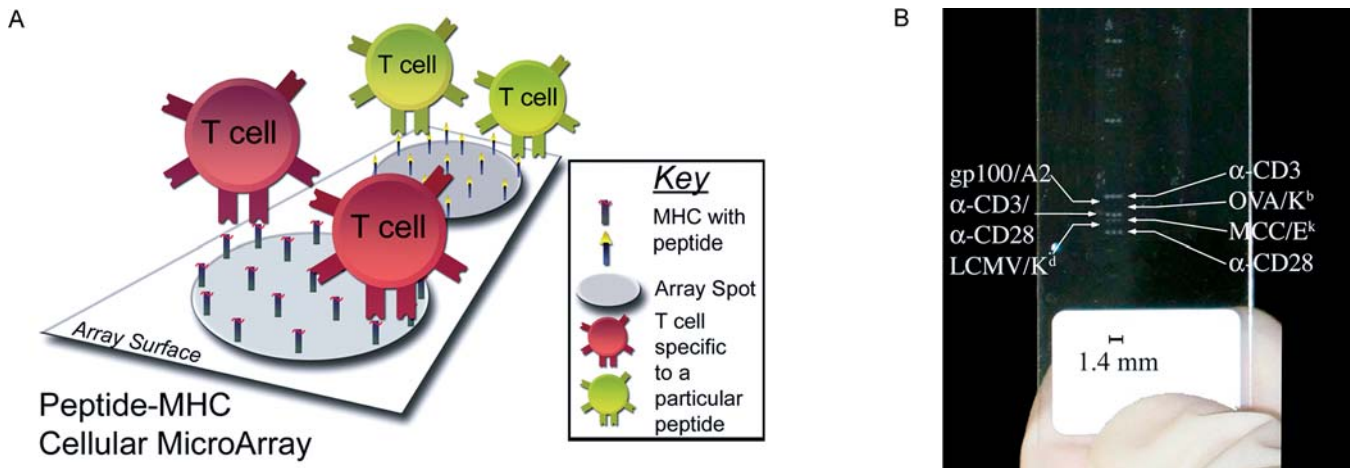


**Figure 1.** A Cellular Microarray

(A) A schematic diagram illustrating T cell binding to its cognate peptide-MHC spot via peptide-MHC-TCR interactions (not drawn to scale). (B) Cells immobilized on the cellular microarray are immediately visible to inspection. When cell coverage exceeds approximately 20% confluency, the cluster becomes visible to the naked eye. Shown are cell clusters bound to several triplicate spots of either peptide-MHC complexes or antibodies. The image was taken using a digital camera. The arrows and legends indicate the locations and identities of each of the printed triplicates. Spot diameter and interspot distance are about 400  $\mu\text{m}$  and 700  $\mu\text{m}$ , respectively. Scale bar is 1.4 mm in length.  
DOI: 10.1371/journal.pbio.0000065.g001

obtained), the cells were washed twice in RPMI and the slide was scanned.

As expected, the resulting differential binding pattern was primarily dictated by antigen specificity even in the presence of a very large excess of nonspecific cells in the suspension. In particular, the preferential binding of a sufficient number of

OT-1 cells to the OVA tetramer (on both top and bottom panels in Figure 3A), together with the absence of OT-1 binding to the LCMV tetramer, demonstrates the feasibility of detecting as few as 0.1% of antigen-specific T cells. Increasing the total cell number (10-fold increase is easily achieved) and using  $\text{CD8}^+$  instead of  $\text{CD11b}^-$  selection should lead to further improvement in sensitivity (data not shown). To test our ability to detect rare T helper cells specific for a selected peptide-class II MHC, DiD-labeled 5c.c7 MCC-specific lymphocytes were diluted to 1% abundance in syngeneic, DiO-labeled B10A splenocytes (Figure 3B) and incubated at 37°C for 10 min. Despite the low percentage of 5c.c7 lymphocytes in the mixture (as reflected by the binding to the anti-CD28 spot in the bottom right panel of Figure 3B), many cells were bound to the MCC/E<sup>k</sup> spots and almost all of them were indeed found to be 5c.c7 cells (Figure 3B, right). In a control experiment on a duplicate array without the 5c.c7 cells, none of the splenocytes adhered to the MCC spots. Taken together, these results show that both class I and II peptide-MHC complexes can be used to detect rare T cell specificities in a complex cell population.

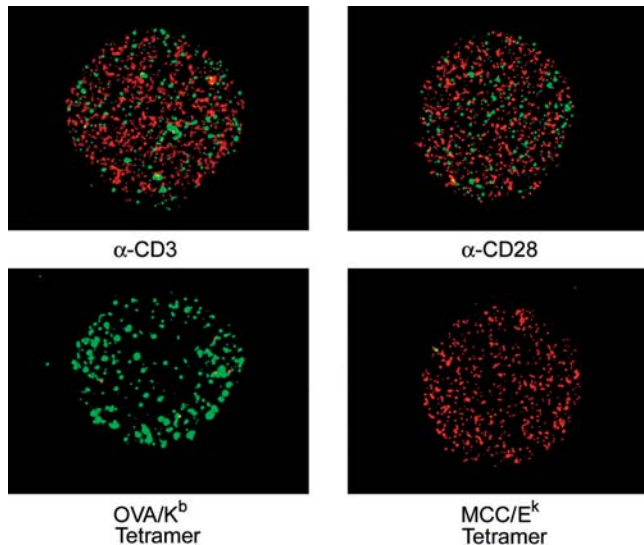


**Figure 2.** Specificity of Lymphocyte Immobilization by Peptide-MHC Arrays

Prelabeled, OVA-specific OT-1 (green) and MCC-specific 5c.c7 (red) lymphocytes ( $6 \times 10^5$ ) were mixed at a 1:1 ratio and added to the preprinted peptide-MHC array. While anti-CD3 and anti-CD28 mAb spots (left and right top panels) immobilize both lymphocyte populations, the OVA and MCC tetramers (left and right bottom panels) capture only the OVA-specific and MCC-specific cells, respectively. Cells were labeled with DiO and DiD lipophilic tracers that incorporate into the cell membrane and do not affect the specificity of cell capture. The printed peptide-MHC tetramer spots contain the fluorescent dye, which allows visualization of peptide-MHC spot borders (data not shown).  
DOI: 10.1371/journal.pbio.0000065.g002

### Detection of a Rare OVA-Specific T Cell Population in Vaccinated C57BL/6 Mice

An important potential application of this technology is in systematically monitoring the T cell repertoire in vivo and its response to immunization, infection, and other stimuli. We tested the feasibility of detecting a weak immune response by monitoring the response of C57BL/6 mice to vaccination with OVA (Figure 4).  $\text{CD8}^+$  lymphocytes ( $2 \times 10^6$  and  $3.2 \times 10^6$ ) from the OVA-vaccinated and mock-vaccinated mice, respectively, were incubated separately with duplicate peptide-MHC arrays (on the same slide) containing OVA/k<sup>b</sup> tetramer, LCMV/k<sup>d</sup> (control) tetramer, and various antibodies. The arrays were incubated at room temperature for 30 min and then washed with RPMI to remove free-floating cells. The cells were also analyzed by flow cytometry after staining with anti-CD8-fluorescein isothiocyanate (FITC) mAb and OVA/k<sup>b</sup>

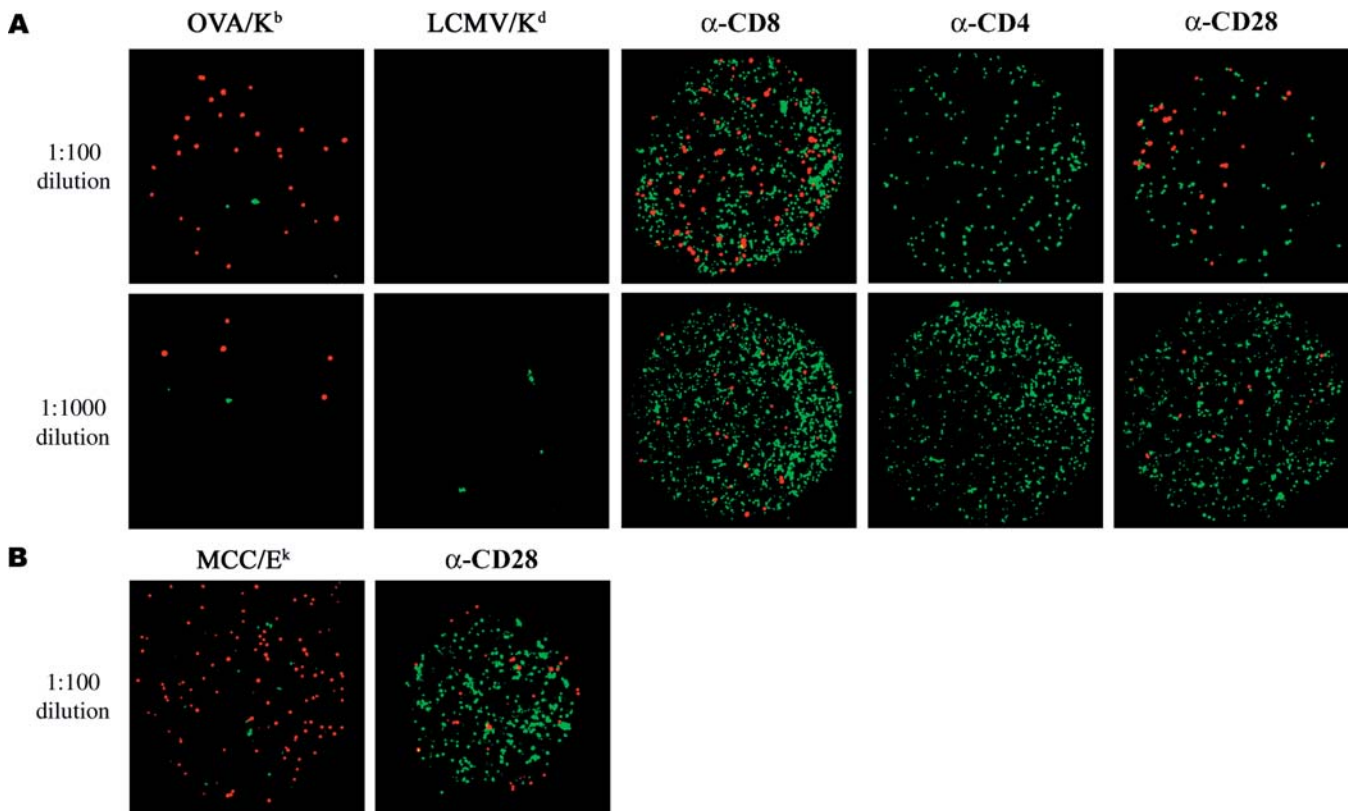


**Figure 3.** Sensitivity of Peptide–MHC Tetramer-Mediated Detection of OVA-Specific CTLs and MCC-Specific Helper T Cells

(A) DiD-labeled OT-1 OVA-specific cells (red) were diluted 1:100 (top panels) or 1:1,000 (bottom panels) in DiO-labeled, monocyte-depleted C57BL/6 mouse lymph node cells (green). DiD-labeled OT-1 cells of  $2.7 \times 10^4$  (top panels) and  $4.41 \times 10^3$  (bottom panels) were mixed, respectively, with  $2.7 \times 10^6$  and  $4.41 \times 10^6$  of DiO-labeled CD11b-depleted lymph node cells. The different dilutions were applied to identical but separate arrays printed with the OVA/K<sup>b</sup> tetramer, the LCMV/K<sup>d</sup> control tetramer, and three different antibody spots (mouse anti-CD8, mouse anti-CD4, and mouse anti-CD28). Following 10-min incubation at 37°C, the cells were washed in RPMI and the slide was scanned. Shown are the OT-1 (red) and lymph node (green) cells that were captured by the OVA tetramer (left), LCMV tetramer (second left), and the antibody spots. (B) Class II MHC-mediated detection and sorting of helper T cells. DiD-labeled 5c.c7 lymphocytes ( $3.5 \times 10^4$ ) (red) were diluted 100-fold in  $3.6 \times 10^6$  B10A DiO splenocytes (green). The mixed suspension was incubated at 37°C for 10 min prior to wash with RPMI. Shown are the 5c.c7 cells (red) and splenocytes (green) captured by the MCC (left) and anti-CD28 (right) spots.  
DOI: 10.1371/journal.pbio.0000065.g003

streptavidin (SA)–PE tetramer. FACS analysis revealed that a small fraction (0.27%) of the CTLs from the vaccinated mouse are OVA-specific, whereas the control mouse did not exhibit an OVA-specific response (Figure 4B). A small but significant number of cells from the OVA-vaccinated mouse were captured on the OVA/K<sup>b</sup> spots, while none were bound by the LCMV/K<sup>d</sup> tetramer spot (Figure 4A). Cells from the mock-vaccinated mouse did not bind to either of the peptide–MHC tetramers. These results demonstrate that these arrays can provide a way to detect even very weak immune responses in normal mice. The ability to use this approach to detect postvaccination populations of peptide-specific T cells in wild-type immune responses has been further confirmed with different peptide–MHC systems (unpublished data).

#### Specific Activation of Lymphocytes Bound to a Peptide–MHC Array Spot

The ability to observe highly specific interactions between live lymphocytes and arrays of proteins raises the possibility of conducting systematic parallel studies of responses to diverse signals arrayed on the surface. We therefore tested

the possibility of using a protein array to investigate dynamic responses of lymphocytes to diverse signals, including specific peptide–MHC complexes and other receptor-specific binding molecules. OT-1 lymphocytes were loaded with the calcium-sensitive dye Fura-2 and were subsequently exposed to an MHC array containing OVA/K<sup>b</sup>, LCMV/K<sup>d</sup>, MCC/E<sup>k</sup>, anti-CD3, anti-CD28, and anti-CD3/anti-CD28 spots. Throughout the experiment, the array was kept at 37°C and 5% CO<sub>2</sub>, and intracellular calcium levels were monitored every 30 s by measuring the ratio of the fluorescence intensity at 340 nm and 380 nm. Binding of OT-1 lymphocytes to the OVA/K<sup>b</sup>, anti-CD3, and anti-CD3/anti-CD28 MHC array spots, but not to LCMV/K<sup>d</sup>, MCC/E<sup>k</sup>, or anti-CD28, led to transient spikes in intracellular calcium levels (Figure 5).

#### Discussion

Cellular immune responses to pathogens, allergens, deregulated or mutated proteins, and self-antigens play critical roles in health and disease. The ability of T cells to respond to the immense diversity of possible targets relies on the corresponding diversity of the repertoire of TCRs that can

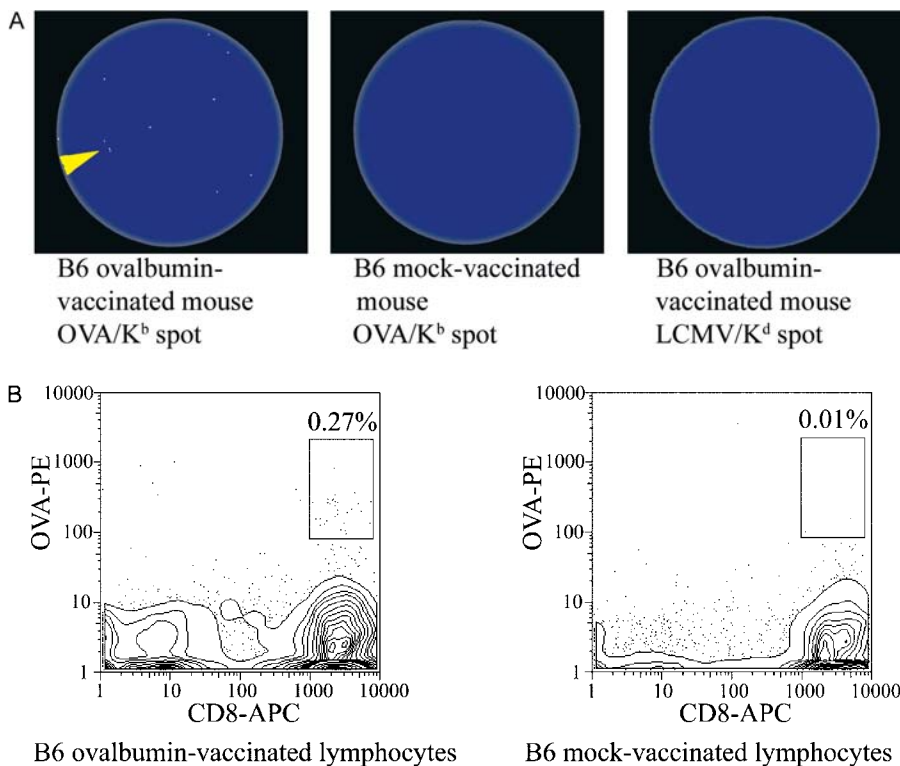


**Figure 4.** Detection of a Weak Immune Response to Vaccination

CTLs from OVA-vaccinated and mock-vaccinated mice were analyzed in parallel using an MHC array and flow cytometry analysis. Mice received base-of-tail injections of OVA/Freund's adjuvant emulsions or PBS (mock)/Freund's adjuvant on day 0 and day 7. Draining lymph nodes were harvested on day 11, and dissociated into a single-cell suspension. (A) CTLs were enriched on an anti-CD8-bead column. Cells ( $2 \times 10^6$  and  $3.2 \times 10^6$ ) from the OVA- and mock-vaccinated mice, respectively, were incubated on identical but separate arrays printed with OVA/ $K^b$  tetramer, LCMV/ $K^d$  (control) tetramer, and various antibodies. The three panels show the relevant array results. A rare population of cells from the OVA-vaccinated mouse was captured on the OVA/ $K^b$  (left), but not on the LCMV/ $K^d$  (right), tetramer spot. The cells captured on the OVA/ $K^b$  tetramer spot were  $CD8^+$  (as determined by counterstaining using an anti-CD8-FITC mAb on the array). An arrowhead points to some of the cells that were bound to that spot. The cells from the mock-vaccinated mouse did not bind the OVA tetramer (middle spot) or the LCMV/ $K^d$  tetramer (data not shown). Spot regions are marked with a blue color by overlaying the tetramer's PE fluorescent signal onto the DIC image.

(B) FACS analysis of the cells from the OVA-vaccinated (left panel) and mock-vaccinated mice (right). Of the total  $CD8^+$  cells from the vaccinated mouse, 0.27% co-stain with OVA/ $K^b$ , compared with 0.01% in the mock-vaccinated mouse.

DOI: 10.1371/journal.pbio.0000065.g004

be generated by the immune system. The T cell population in each individual is diverse and dynamic. Even after exposure to a potent T cell antigen, an individual TCR clone seldom accounts for more than 5% of the total population of T cells in a normal human or mouse. Moreover, the specificities and phenotypes of the individual's T cell repertoire may provide a rich picture of the immunological history, the physiological status, and perhaps the disease susceptibilities of that individual. A broad picture of the dynamic responses of the T cell repertoire to an immunological challenge should illuminate our understanding of the immune response and may point to individual-specific response patterns that can help guide design of immunological therapies.

The development of peptide–MHC tetramers (Altman et al. 1996) and variations (Greten et al. 1998) as staining reagents has greatly aided the analysis of antigen-specific populations of CD4 and CD8 T cells. Unfortunately, the number of specificities that can be analyzed is severely limited by the fluorescence spectra available for conjugation to individual peptide–MHC complexes.

Furthermore, the complex compensation required for multiple fluorophores and numerous controls required for adequate tetramer staining, such as a control tetramer, propidium iodide for dead cell staining, anti-CD8, anti-CD11, anti-CD19, and anti-CD56, further restrict the ability

to analyze multiple specificities simultaneously. Hence, analyzing more than a few specificities is difficult and is impractical for a typical clinical sample. By using specified, predetermined spatial coordinates rather than fluorescent tags, microarray technology has revolutionized the analysis of gene and protein expression, allowing the simultaneous analysis of hundreds to thousands of different variations in gene and protein expression. This approach has been recently used to analyze intact cells (Belov et al. 2001; Brown et al. 2003), allowing the simultaneous characterization of hundreds of cell surface molecules, by applying a homogeneous population of cells to an array of mAbs. We have extended the experimental logic of that approach to the characterization and isolation of antigen-specific populations of T cells from a heterogeneous cell mixture. Furthermore, cospotting peptide–MHCs with other effector molecules and/or co-culturing the T cells with other effector cells may allow for high throughput examination of MHC presentation in the context of other molecular signals and might open exciting avenues for antigen-specific intercellular interaction assays. Together, these methods should provide an efficient approach to epitope discovery and broad, systematic characterization of TCR specificity and the relations between epitope recognition and T cell activation, reactivity, anergy, and cell death.

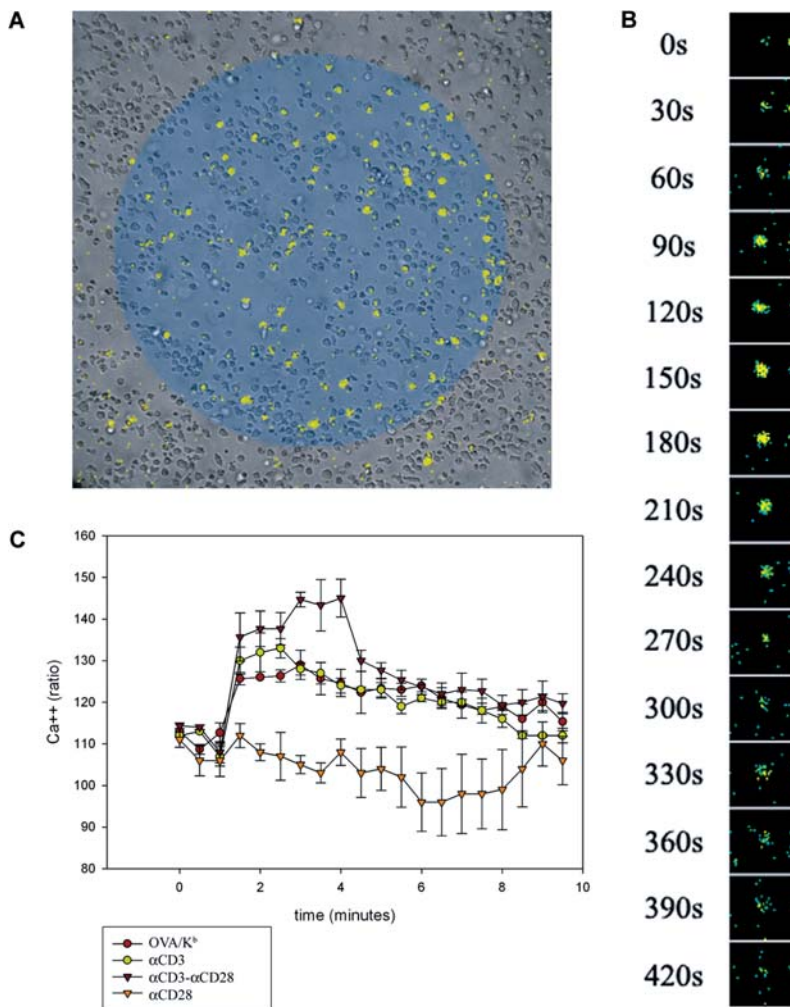


**Figure 5.** Activation of OT-1 Lymphocytes Following an Exposure to Preprinted Spots on an MHC Array

OT-1 lymphocytes were preloaded with Fura-2 dye for 20 min at room temperature prior to exposure to the cellular microarray (time 0). The cells were incubated at 37°C, 5% CO<sub>2</sub>, and fluorescence intensities at 340 nm and 380 nm were measured every 30 s from each of the spots on the array. Calcium flux signal was triggered in the OVA-specific cells as soon as they reached the OVA/K<sup>b</sup> tetramer spots, the activating antibody spots (anti-CD3 and anti-CD3/anti-CD28), but not the irrelevant MCC/E<sup>k</sup> tetramer or the nonactivating antibody spots (e.g. anti-CD28).

(A) Calcium flux signal (yellow) overlaid onto a 10x DIC image of OT-1 cells on a combined FITC-labeled anti-CD3/anti-CD28 spot. Fura-2 fluorescence intensity ratios are represented in pseudo-color, and the overlaid spot region (blue) is determined from the FITC image. Note that the spot pattern can be inferred from the Fura-2 signal representing activation, even without removing unbound cells.

(B) A time-lapsed series of images taken of a representative OT-1 lymphocyte specifically immobilized onto an OVA/K<sup>b</sup> spot. The cell undergoes a rapid, transient calcium flux as measured by Fura-2 fluorescence.

(C) Averaged calcium flux traces ( $n = 3$ ) recorded from an OVA/K<sup>b</sup> spot (purple circles), anti-CD3/anti-CD28 spot (brown triangles), anti-CD3 spot (green circles), and nonactivating anti-CD28 spot (orange triangles). Error bars represent calculated standard error of mean.

DOI: 10.1371/journal.pbio.0000065.g005

The excellent performance of peptide–MHC complexes as binding probes in our cellular microarray format is somewhat surprising because the typical TCR affinity is about  $10^3$ - to  $10^4$ -fold lower than that of a typical mAb and its antigen (Davis et al. 1998). Still, sufficient numbers of peptide–MHC complexes bound to a given cell can compensate for relatively low affinity of a single peptide–MHC–TCR interaction. In fact, a simple order of magnitude calculation shows that for a typical peptide–MHC concentration, as few as approximately 200 peptide–MHC–TCR interactions are sufficient to capture and stably hold a cell against typical flow forces experienced during the washing of unbound cells (an example of this calculation is provided in the Supporting Information section).

The combination of large spots on an inert substrate allows the reliable detection of as few as three to five bound cells per spot. For cells with a diameter of 10  $\mu\text{m}$  on a 400  $\mu\text{m}$  spot, this corresponds to a dynamic range of about 300-fold, which can be further increased using larger spot sizes (i.e., dispensing more drops on each spot) or using multiple spots of the same size. More importantly, since rare populations of cells can be detected only when a sufficient number of them encounter the appropriate probe region, the total probe area (i.e., surface area of one spot multiplied by the number of

identical spots) has a major effect on the sensitivity. We have shown that the limit of detection with a single 400  $\mu\text{m}$  spot of a weak model antigen is about 0.1% (i.e., one positive out of 1,000 cells). Increasing the number of identical spots results in an improvement in sensitivity, the extent of which is under investigation. Further improvement might be achieved by increased exposure of cells to each MHC-printed region (e.g., by sample agitation, reloading, or directed flow). Another route towards a significant improvement in both sensitivity and signal-to-noise ratio is cell enrichment prior to MHC array analysis. For example, preselection of CD8<sup>+</sup> or CD4<sup>+</sup> from peripheral blood mononuclear cells (e.g., by bead selection or FACS sorting) results in approximately a 10-fold enrichment of specific target cells and eliminates the nonspecific binding of a subpopulation of CD11b<sup>+</sup> cells to MHC spots. Further enrichment via negative and/or positive selection using common markers would almost certainly extend the lower limit of partial abundance required for detection.

The number of cells captured on the array depends on the abundance of cells expressing the appropriate TCR, its expression level, and affinity to the peptide–MHC complex, the concentration, functionality, and accessibility of that complex, and several other factors, including the local cell

density, incubation, and washing conditions, local film, integrity etc. Consequently, estimating the frequency of cells expressing a given antigen specificity requires the development of a standardized protocol. One possible approach is to coexpose differentially labeled cell populations to the same spots using a standard pool of T cells as a common internal standard in each analysis, analogous to the reference RNA commonly used for DNA microarray studies of gene expression (Eisen and Brown 1999). The use of a common internal standard can provide a way to eliminate local spot- and slide-dependent factors and obtain a relative measure for the number of cells that are above the threshold for functional binding, allowing quantitative differential profiling of cell surface markers based on the relative number of bound cells.

The use of printed arrays of specific binding reagents for characterizing populations of cells has similarities to FACS in concept and applications. FACS has the advantage of allowing analysis on a cell-by-cell basis, while the cellular microarray approach allows a much larger number of molecules to be analyzed in a population of cells. Currently, a single cellular microarray can accommodate more than 1,000 peptide–MHC probes (without decreasing the spot size), which allows detection of 1,000 antigen-specific cell populations in a single assay. Each cellular microarray-based assay is easy to perform, utilizes fixed gating that eliminates the subjective gating of FACS-based analysis, and allows many samples to be analyzed side by side either on the same slide (for small arrays) or on different slides. The high throughput should make it practical to screen a sample population of cells (e.g., from a patient) against a large panel of candidate peptide–MHC complexes or to discover novel MHC-restricted epitopes by screening libraries of random, mutated, and chemically modified sequences. Although the fractional abundance of specific T cells required for detection in our experiments (0.1%) is not as low as can be detected in the best FACS analyses (0.01%), it is already sufficient to identify an immune response of clinical relevance and is likely to improve with further optimization.

What are the prospects for efficient array-based detection of immune responses and characterization of the TCR recognition and activation landscape? The actual set of TCR specificities and sensitivities, at any given time, depends on the history of exposure to antigens, genotype, and the physiological parameters. We have shown that a physiologically relevant response to an antigen challenge is detectable as cell capture by the cognate peptide–MHC (see Figure 4). Since an expanded population of activated T cells may cross-react with epitopes having a considerable degree of sequence homology (Reay et al. 1994; Wucherpfennig and Strominger 1995; Kersh and Allen 1996; Bach et al. 1998; Honeyman et al. 1998; Mason 1998; Zhao et al. 1998; Hiemstra et al. 1999; Misko et al. 1999), a signature of binding to multiple peptides is also possible, especially for structurally similar epitopes (high surface concentration of the peptide–MHC may further contribute to the ability to capture cross-reacting T cells). Moreover, in numerous important pathologies associated with both specific and nonspecific polyclonal activation of the host immune system, the binding of activated clones to many unrelated (and often self-protein-derived) peptides is very plausible. For example, a single cancer patient can develop immune responses to multiple tumor-associated

antigens (Rosenberg 2001). In one case, tumor-infiltrating lymphocytes from a single patient recognized tyrosinase (a differentiation antigen presented by human leucocyte antigen [HLA] class I),  $\beta$ -catenin (a class I mutation), p15 (a class I antigen involved in posttranscriptional control), gp100 (a class I intronic sequence and class II normal sequence), tyrosinase-related protein-1 (TRP-1, a class II differentiation antigen), TRP-2 (a class II differentiation antigen), and Ki-67 (a class II mutation).

The wide range of specificities against nonhomologous antigens demonstrated in this and other reports strongly supports the feasibility of cellular microarray-based characterization of patient-specific immune response patterns. An example for a nonspecific, clinically important response is a superantigen-induced stimulation, which often leads to a massive polyclonal lymphocyte activation that might account for up to 30% of the host T cell repertoire (depending on the number of  $V_{\beta}$  families capable of interacting with the superantigen) (Muller-Alouf et al. 2001). Still, while the cellular microarray should be sensitive enough to identify and examine binding patterns in activated samples, its ability to characterize the naive repertoire might be limited. This drawback may be mitigated by modifying the geometry of the array and/or the sample introduction method so as to increase the chances of rare cell populations encountering each of the peptide–MHC complexes.

Taking advantage of the full potential of this approach requires convenient means for synthesizing diverse arrays of peptide–MHC complexes. Conventional MHC tetramer synthesis is cumbersome and technically difficult, making the effective implementation of large, functional peptide–MHC libraries a practical challenge. However, usage of reloadable MHC constructs such as DimerX (BD Biosciences) or the MHC tetramer-based Epitope Discovery System (Beckman Coulter) should allow for an efficient production of printable MHC molecules loaded with diverse peptide epitopes of interest. Indeed, preliminary experiments suggest that the DimerX peptide-loadable reagent has a similar specificity and sensitivity to that of peptide–MHC tetramers.

The experimental strategy introduced here provides a powerful tool for simultaneous detection and study of antigen-specific T cell populations. This technique can be performed rapidly (10 min), requires little technical expertise, and allows screening of a single clinical sample (with  $CD4^{+}$  and/or  $CD8^{+}$  T cells) against a library of specific or random peptide–MHCs. Although the data presented here were generated using cells derived from mice, preliminary results indicate that this approach works equally well with human samples. Numerous clinically significant MHC-restricted epitopes have already been defined. These can be easily printed on a single microarray to provide a rapid test for the cognate T cell responses and to study the involvement of multiple epitopes during the course of a disease or following vaccination. Co-immobilization with effector molecules and cells may assist in identifying key factors that take part in the regulation of T cell effector function. Thus, the development of peptide–MHC cellular microarrays should provide valuable insights into dynamic and individual variations in the global repertoire of T cell specificities and the mechanisms that control them.

## Materials and Methods

**Peptides and cell lines.** MCC 88–103 (ANERADLIAYLKQATK), OVA 258–265 (SIINFEKL), HIV gag 77–85 (SLYNTVATL), and LCMV gp1 33–41 (KAVYNFATC) peptides have been produced at the Protein and Nucleic Acid Facility at Stanford University (Stanford, California, United States).

OT-1 TCR transgenic mice (Hogquist et al. 1994) bred into a wild-type C57BL/6 background (Fazekas de St. Groth et al. 1993), expressing homozygous for MHC class I-restricted OVA-specific TCR, were a generous gift from Dr. Stephen Schoenberger (San Diego, California, United States). 5c.c7 are TCR transgenic mice expressing homozygous for MHC class II MCC-specific TCR. Animals were housed in a pathogen-free condition.

**Peptide–MHC class I tetramer preparation and staining.** This technique was developed in the Davis lab (Altman et al. 1996) and has been widely used. In brief, a 15 amino acid linker/BirA substrate peptide (BSP) for BirA-dependent biotinylation has been genetically engineered onto the COOH terminus of the mouse H-2K<sup>b</sup> or I-E<sup>k</sup> gene. The MHC class I/BirA substrate peptide fusion protein was expressed in *Escherichia coli* with  $\beta_2$ -microglobulin and folded in vitro with specific peptide ligands. The properly folded peptide–MHC class I– $\beta_2$ -microglobulin complex was then extensively purified and biotinylated on a lysine residue within the BSP using the BirA enzyme (Avidity, Denver, Colorado, United States). Tetramers were produced by adding to biotinylated peptide–MHC complexes PE–SA (Prozyme, San Leandro, California, United States) at a molar ratio of 4:1. Specificity is demonstrated by lack of staining in irrelevant CTLs. Tetramers were individually titrated and used at the optimum concentration based on signal-to-noise ratio, usually 10  $\mu$ g/ml. LCMV/K<sup>d</sup> was purchased from Beckman Coulter (Allendale, New Jersey, United States). Cells ( $1 \times 10^6$ ) were stained with the specific tetramer of interest for 30 min at 4°C. Antibodies were then added at the recommended concentrations and incubated for 30 min at 4°C.

**Preparation of MHC and antibody arrays.** The following MHC tetramers and antibodies were prepared in a v-shaped 384-well plate (Genetix Pharmaceuticals, Cambridge, Massachusetts, United States) with approximately 12  $\mu$ l per well: (i) a 2-fold dilution series of OVA/H-2K<sup>b</sup> tetramer (1 to 1:16X, with 1X concentration being 0.17 mg/ml), (ii) gp100/HLA-A2 tetramer (at 0.52 mg/ml), (iii) MCC/I-E<sup>k</sup> tetramer (0.42 mg/ml), (iv) LCMV/H-2K<sup>d</sup> tetramer (Beckman Coulter) at 0.33 mg/ml, (v) mouse anti-CD3 mAb (clone 17A2; BD Pharmingen, San Diego, California, United States) at 0.5 mg/ml, (vi) mouse anti-CD28 mAb (clone 37.51; BD Pharmingen) at 0.5 mg/ml, and (vii) a 1:1 mixture of mouse anti-CD3 and mouse anti-CD28 (each at a final concentration of 0.25 mg/ml). Each of the tetramer and DimerX solutions were supplemented with 2% glycerol. All samples were arrayed in triplicates onto three-dimensional substrates comprised of microscope slides coated with a polyacrylamide gel (Perkin Elmer, Boston, Massachusetts, United States). Slides were processed for printing according to the manufacturer's instructions, and the samples were then dispensed with a noncontact piezo-electric arrayer (Perkin Elmer). About 4.5 nl of sample (10 drops of approximately 0.45 nl) were dispensed on each spot (approximately 400  $\mu$ m in diameter). To allow for more than one independent assay on each slide, each of the samples (or, in some cases, part of the samples) was dispensed in two groups (or blocks) with an intergroup distance of 5 mm. Following the print run, the arrayed proteins were immobilized within the gel substrate by incubating the slides for 24 h at 4°C in a humid chamber. Following the immobilization, the arrays were placed in a dry slide box, sealed with tape, and stored at 4°C until used. Stored slides were used for 5 mo without an observed reduction in activity or diffusion of the spotted constructs (lack of diffusion was determined by examining the diameter of the PE-labeled MHC tetramer spots as viewed by fluorescence microscopy).

**Array panning.** OT-1 and 5c.c7 transgenic mice were sacrificed on day 0 by cervical dislocation. Axillary and inguinal lymph nodes were harvested and a single-cell suspension obtained by straining through a 70- $\mu$ m cell strainer (BD Falcon, San Diego, California, United States) in RPMI fortified with 10% fetal calf serum (FCS), penicillin, streptomycin, glutamine,  $\beta$ -mercaptoethanol, and nonessential amino acids. OVA or MCC peptide (1  $\mu$ M) was then added and the cells were incubated at 37°C. On day 1, murine IL-2 (Sigma, St. Louis, Missouri, United States) was added to the lymphocytes to a final concentration of 30 U/ml. On days 7–10, lymphocytes were suspended in RPMI (deficient in phenol red) with 5% FCS at a concentration of  $10^4$ – $10^8$  cells/ml prior to incubation on the peptide–MHC tetramer array. B10A or C57BL/6 mice were sacrificed, and single-cell splenocyte suspensions was subjected to a Ficol gradient and CD11b<sup>−</sup> depletion (Miltenyi Biotec, Bergisch Gladbach, Germany) prior to being used as

syngeneic controls. Cells were labeled with fluorescent lipophilic tracers DiO, DiD, and DiI (Molecular Probes, Eugene, Oregon, United States) according to the manufacturer's instructions. Labeled or unlabeled cells were directly added to the peptide–MHC array by gentle layering in volumes of 20–50  $\mu$ l. The array was incubated either at 37°C or 20°C for 10–30 min. Following incubation, the array was washed twice with RPMI to remove unbound cells. (For more detailed information, see Protocol S1.)

**Detection of a weak postvaccine immune response.** MHC arrays were used to monitor CD8-specific immune responses to OVA vaccination in wild-type C57BL/6 mice. Mice received base-of-tail injections of 1:1 OVA (100  $\mu$ g in 100  $\mu$ l of phosphate-buffered saline [PBS]; Sigma)/Freund's adjuvant (Sigma) emulsions or PBS/Freund's adjuvant (mock vaccination) on day 0 and day 7. Mice were sacrificed on day 11 and underwent anti-CD8<sup>+</sup> selection (Miltenyi Biotec) from single-cell suspensions derived from mouse lymph nodes. CD8<sup>+</sup> lymphocytes from both OVA- and mock-vaccinated mice were applied to separate MHC arrays. FACS analysis of the same population of cells was performed as detailed above, with anti-CD8-FITC mAb, OVA/K<sup>b</sup> SA-PE tetramer, and an HIV gag 77–85/HLA-A\*0201 SA-PerCP dump tetramer. FACS analysis was performed on a Becton Dickinson LSR at the Stanford University FACS Facility (Stanford, California, United States).

**Intracellular calcium measurements.** To determine whether the MHC array could be used to probe intact lymphocyte activation pathways, OT-1 lymphocytes were loaded with 5  $\mu$ g/ml calcium-sensitive dye Fura-2 (Molecular Probes) for 20 min at room temperature. The lymphocytes were then exposed to an MHC array containing OVA/K<sup>b</sup>, LCMV/K<sup>d</sup>, MCC/E<sup>k</sup>, anti-CD3, anti-CD28, and anti-CD3/anti-CD28 spots. Intracellular calcium levels were monitored every 30 s by measuring the ratio of the fluorescence intensity at 340 nm and 380 nm using the fluorescence microscopy equipment detailed below.

**Array imaging.** Imaging was performed using a Zeiss (Oberkochen, Germany) Axiovert-100TV microscope and a Fluor 10x fitted with a high-speed piezo-electric z-motor (Physik Instruments, Downingtown, Pennsylvania, United States), Princeton Instruments liquid-cooled CCD Interline camera (Roper Scientific, Trenton, New Jersey, United States), and dual excitation and emission filter wheels (Sutter Instruments, Novato, California, United States). A DIC image, a Cy3 (for DiI or PE), a Cy5 (DiD) and/or a FITC (DiO) image, and/or 340 nm and 380 nm images were collected every 30 s for up to 1 h. Microscope control, acquisition of data, and image analysis were performed using Metamorph (Universal Imaging, Downingtown, Pennsylvania, United States).

## Supporting Information

To evaluate the effect of tetramer dilution on cell capture, we printed an OVA/k<sup>b</sup> tetramer dilution series and probed it with OT-1 cells (Figure S1A). The cells were suspended at  $2.5 \times 10^6$  cell/ml ( $10^5$  cells in 40  $\mu$ l), which was below the concentration required for confluent coverage of the spot area. The cells were then incubated with the array (30 min at room temperature) and imaged following washout of unbound cells. In this specific example, the number of cells captured increased linearly with the amount of tetramer deposited (Figure S1B), with a binding threshold of approximately 0.05 ng/spot. The lack of plateau at high tetramer concentrations, together with the denser cell coverage on the anti-CD3 spots, suggests that a still further increase in tetramer concentration (without changing the suspension density) would result in higher numbers of bound cells. Indeed, a 4-fold increase in the amount of tetramer deposited leads to a significant increase in binding efficiency, which becomes comparable to binding via a mAb (data not shown). The lack of cell binding between spots or to noncognate peptide–MHC spots indicates that binding of as low as a few cells is attributable to peptide–MHC–TCR recognition. Note, however, that the linear shape of the binding curve (Figure S1B) should be considered as a special case and not as a general rule. Likewise, the minimal concentration for binding depends on the availability and functionality of the immobilized peptide–MHC, the peptide–MHC–TCR affinity, the type, density, and heterogeneity of the cells, the incubation temperature and duration, and the stringency of washing.

In general, the binding curve should depend on the immobilization kinetics, the heterogeneity in TCR expression level, and its affinity to the peptide–MHC complex. For a sufficiently dense, homogeneous cell suspension, we expect to find a sigmoidal binding curve with a sharp transition from no binding to a plateau at some critical tetramer concentration. Indeed, in some other peptide–MHC–TCR

systems (and higher suspension densities), the binding curve has a sigmoidal shape (data not shown). Heterogeneity in TCR affinity and expression level should lead to a less steep increase in captured cell number as a function of surface ligand density. Therefore, the linear binding curve (Figure S1B) probably reflects a wide distribution of TCR expression levels and/or affinities and should not be considered as a pure statement on binding kinetics. Still, an exact linear curve is somewhat surprising.

The excellent performance of peptide–MHC complexes as binding probes in an array format was somewhat surprising because the typical TCR affinity is about  $10^3$ - to  $10^4$ -fold lower than that of a typical mAb and its antigen (Davis et al. 1998). Still, sufficient numbers of peptide–MHC complexes bound to a given cell can compensate for relatively low affinity of a single peptide–MHC–TCR bond. By incorporating kinetic parameters specific to the OT-1/OVA tetramer interaction into a simplified adhesion model proposed by Bell (1978), the actual number of OT-1/OVA/ $K^b$  tetramer bonds can be estimated as follows. Each spot typically contains approximately  $2 \times 10^{10}$  tetramers, corresponding to a maximal surface concentration of about  $1.5 \times 10^{13}/\text{cm}^2$ . Since the tetramers are deposited into a three-dimensional film, and some of them may lose their functionality during the deposition and thereafter, the actual surface concentration may be significantly smaller. Assuming that only about 1% of the tetramers are actually available for binding, the critical force per bond, above which a cell cannot be stably bound to the surface (Bell 1978), is given by  $f_c \approx 6 \times 10^{-12} \times \ln(N_s/K_D^{(2d)}) \approx 35\text{pN}$ /bond, where  $N_s$  is the effective surface concentration of the tetramer and  $K_D^{(2d)}$  is the estimated two-dimensional dissociation constant between the OT-1 TCR and a single OVA/MHC tetramer ( $K_D^{(2d)}, \sim 4 \times 10^8$  molecules/ $\text{cm}^2$ ).

For medium viscosity  $\eta = 7 \times 10^{-3}$  g/(cm/s) and cell radius  $a = 3 \mu\text{m}$ , the hydrodynamic Stokes force,  $F$ , exerted by a constant flow during washout of unbound cells is given by  $F = 6\pi\eta av$ , where  $v$  is the velocity of the slide as it moves through the washing medium. Hence, for a typical washing velocity of 10 cm/s, the detaching force  $F = 4\text{nN}$  may be compensated by as few as 114 OT-1/OVA tetramer bonds. Assuming an interaction area of  $15 \mu\text{m}^2$ , the surface concentration of bound OT-1 TCRs at the time of washing must be higher than  $7.6/\mu\text{m}^2$ . Such surface density can be easily achieved even for a uniform TCR surface distribution. For example, for a T cell of radius  $a$ , having a uniform TCR distribution, a surface density of  $7.6/\mu\text{m}^2$  corresponds to a total of 382 TCRs. In a typical OT-1 cell, the TCR expression level is about two orders of magnitude higher than this lower bound. A more realistic scenario of TCR recruitment to the “artificial immunological synapse” (resulting in a nonuniform TCR distribution) would correspond to an even lower bound.

Thus, given the relevant physiological and kinetic parameters (incorporated into a simplified adhesion model), the major determinant of cell capture is the surface density,  $N_s$ , of functional peptide–MHC complexes. For a sufficiently high  $N_s$ , the critical force per bond,  $f_c$ , is high enough to provide for a stable cell capture with as few as a couple hundred peptide–MHC–TCR bonds. Note that the logarithmic dependence of the critical force on both the peptide–MHC surface concentration and the peptide–MHC–TCR affinity

(which directly influences the  $K_D^{(2d)}$ ) gives rise to a wide range of  $N_s$  and  $K_D^{(2d)}$  values that are compatible with a stable capture.

### Figure S1. Binding of OT-1 Lymphocytes to a Serial Dilution of OVA/ $K^b$ Tetramer

The effect of tetramer dilution on cell capture was tested by examining the binding of OT-1 lymphocytes to a serial dilution of immobilized OVA/MHC tetramer. The cells were suspended at a concentration of  $2.5 \times 10^6/\text{ml}$  and incubated on the array for 30 min at room temperature. Following the removal of unbound cells, the array was imaged and scored for the number of OT-1 cells on each of the spots.

(A) A reconstruction of the relevant array region by a patchwork of  $10 \times$  images, revealing a monotonic reduction in the number of bound cells with tetramer dilution. Amount of MHC tetramer deposited is given in nanograms per spot.

(B) In this specific example, the number of immobilized OT-1 lymphocytes on the OVA/ $K^b$  spots was linearly dependent on the amount of tetramer deposited. Averaged cell numbers and standard errors are based on triplicate spots. The line represents a linear fit to the data.

View online at DOI: 10.1371/journal/pbio.0000065.sg001 (for Figure S1A) (3.89 MB TIFF) and at DOI: 10.1371/journal/pbio.0000065.sg002 (for Figure S1B) (5.83 MB TIFF).

### Protocol S1. Online Protocol for the MHC Cellular Microarray

This protocol serves as a general template for a basic MHC cellular microarray experiment. Depending on the exact goal of a specific experiment, some of the parameters described may require modification.

View online at DOI: 10.1371/journal/pbio.0000065.sd001 (38 KB DOC).

## Acknowledgments

We would like to thank M. Krogsgaard for supplying the MCC/I-E<sup>k</sup> tetramer; J. T. Chi, B. F. Lillemeier, Y. H. Chien, P. J. Ebert, J. B. Huppa, M. Krogsgaard, M. S. Kuhns, Q. Li, M. A. Furhboo, and C. Sumen for scientific discussions. This study was funded by grants from the Howard Hughes Medical Institute, the Human Frontier Science Program, the Pediatric Scientist Development Program, and the National Institutes of Health.

**Conflicts of interest.** The authors have declared that no conflicts of interest exist.

**Author contributions.** YS and DSC conceived and designed the experiments. YS and DSC performed the experiments. YS and DSC analyzed the data. YS, DSC, DLK, MMD, and POB contributed reagents/materials/analysis tools. YS, DSC, MMD, and POB wrote the paper. DLK helped to initially conceive of the work and experiments. YS and DSC should be considered co-first authors on this paper. MMD and POB suggested ideas and experiments. MMD and POB should be considered co-principal investigators and co-corresponding authors on this paper. ■

## References

- Altman JD, Moss PA, Goulder PJ, Barouch DH, McHeyzer-Williams MG, et al. (1996) Phenotypic analysis of antigen-specific T lymphocytes. *Science* 274: 94–96.
- Bach JM, Otto H, Jung G, Cohen H, Boitard C, et al. (1998) Identification of mimicry peptides based on sequential motifs of epitopes derived from 65-kDa glutamic acid decarboxylase. *Eur J Immunol* 28: 1902–1910.
- Bell GI (1978) Models for the specific adhesion of cells to cells. *Science* 200: 618–627.
- Belov L, de la Vega O, dos Remedios CG, Mulligan SP, Christopherson RI (2001) Immunophenotyping of leukemias using a cluster of differentiation antibody microarray. *Cancer Res* 61: 4483–4489.
- Callan MF, Tan L, Annels N, Ogg GS, Wilson JD et al. (1998) Direct visualization of antigen-specific CD8<sup>+</sup> T cells during the primary immune response to Epstein–Barr virus *in vivo*. *J Exp Med* 187: 1395–1402.
- Davis MM, Boniface JJ, Reich Z, Lyons D, Hampl J, et al. (1998) Ligand recognition by alpha beta T cell receptors. *Annu Rev Immunol* 16: 523–544.
- Eisen MB, Brown PO (1999) DNA arrays for analysis of gene expression. *Methods Enzymol* 303: 179–205.
- Fazekas de St. Groth B, Patten PA, Ho WY, Rock EP, Davis MM (1993) An analysis of T cell receptor–ligand interaction using a transgenic antigen model for T cell tolerance and T cell receptor mutagenesis. In: Alt FW, Vogel AH, editors. *Molecular mechanisms of immunological self-recognition*. San Diego, California: Academic Press. pp. 123–127.

- Greten TF, Slansky JE, Kubota R, Soldan SS, Jaffee EM, et al. (1998) Direct visualization of antigen-specific T cells: HTLV-1 Tax11–19-specific CD8(+) T cells are activated in peripheral blood and accumulate in cerebrospinal fluid from HAMTSP patients. *Proc Natl Acad Sci U S A* 95: 7568–7573.
- Haanen JB, van Oijen MG, Tirion F, Oomen LC, Kruisbeek AM, et al. (2000) *In situ* detection of virus- and tumor-specific T cell immunity. *Nat Med* 6: 1056–1060.
- Hiemstra HS, Duinkerken G, Benckhuijsen WE, Amons R, de Vries RR, et al. (1997) The identification of CD4<sup>+</sup> T cell epitopes with dedicated synthetic peptide libraries. *Proc Natl Acad Sci U S A* 94: 10313–10318.
- Hiemstra HS, Benckhuijsen WE, Amons R, Rapp W, Drijfhout JW (1998a) A new hybrid resin for stepwise screening of peptide libraries combined with single bead Edman sequencing. *J Pept Sci* 4: 282–288.
- Hiemstra HS, van Veelen PA, Schloot NC, Geluk A, van Meijgaarden KE, et al. (1998b) Definition of natural T cell antigens with mimicry epitopes obtained from dedicated synthetic peptide libraries. *J Immunol* 161: 4078–4082.
- Hiemstra HS, van Veelen PA, Willemsen SJ, Benckhuijsen WE, Geluk A, et al. (1999) Quantitative determination of TCR cross-reactivity using peptide libraries and protein databases. *Eur J Immunol* 29: 2385–2391.
- Hogquist KA, Jameson SC, Heath WR, Howard JL, Bevan MJ, et al. (1994) T cell receptor antagonist peptides induce positive selection. *Cell* 76: 17–27.
- Honeyman MC, Stone NL, Harrison LC (1998) T cell epitopes in type 1 diabetes autoantigen tyrosine phosphatase IA-2: Potential for mimicry with rotavirus and other environmental agents. *Mol Med* 4: 231–239.



- Ignatowicz L, Kappler J, Marrack P (1996) The repertoire of T cells shaped by a single MHC/peptide ligand. *Cell* 84: 521–529.
- Kersh GJ, Allen PM (1996) Structural basis for T cell recognition of altered peptide ligands: A single T cell receptor can productively recognize a large continuum of related ligands. *J Exp Med* 184: 1259–1268.
- Lee PP, Yee C, Savage PA, Fong L, Brockstedt D, et al. (1999) Characterization of circulating T cells specific for tumor-associated antigens in melanoma patients. *Nat Med* 5: 677–685.
- Mason D (1998) A very high level of crossreactivity is an essential feature of the T cell receptor. *Immunol Today* 19: 395–404.
- Misko IS, Cross SM, Khanna R, Elliott SL, Schmidt C, et al. (1999) Crossreactive recognition of viral, self, and bacterial peptide ligands by human class I-restricted cytotoxic T lymphocyte clonotypes: Implications for molecular mimicry in autoimmune disease. *Proc Natl Acad Sci U S A* 96: 2279–2284.
- Moldrem JJ, Lee PP, Wang C, Felio K, Kantarjian HM, et al. (2000) Evidence that specific T lymphocytes may participate in the elimination of chronic myelogenous leukemia. *Nat Med* 6: 1018–1023.
- Muller-Alouf H, Carnoy C, Simonet M, Alouf JE (2001) Superantigen bacterial toxins: State of the art. *Toxicon* 39: 1691–1701.
- Ogg GS, Jin X, Bonhoeffer S, Dunbar PR, Nowak MA, et al. (1998a) Quantitation of HIV-1-specific cytotoxic T lymphocytes and plasma load of viral RNA. *Science* 279: 2103–2106.
- Ogg GS, Rod Dunbar P, Romero P, Chen JL, Cerundolo V (1998b) High frequency of skin-homing melanocyte-specific cytotoxic T lymphocytes in autoimmune vitiligo. *J Exp Med* 188: 1203–1208.
- Pinilla C, Appel JR, Houghten RA (1994) Investigation of antigen-antibody interactions using a soluble nonsupport-bound synthetic decapeptide library composed of four trillion sequences. *Biochem J* 301: 847–853.
- Reay PA, Kantor RM, Davis MM (1994) Use of global amino acid replacements to define the requirements for MHC binding and T cell recognition of moth cytochrome c (93–103). *J Immunol* 152: 3946–3957.
- Rosenberg SA (2001) Progress in human tumour immunology and immunotherapy. *Nature* 411: 380–384.
- Seneviratne SL, Jones L, King AS, Black A, Powell S, et al. (2002) Allergen-specific CD8(+) T cells and atopic disease. *J Clin Invest* 110: 1283–1291.
- Smith SM, Brookes R, Klein MR, Malin AS, Lukey PT, et al. (2000) Human CD8<sup>+</sup> CTL specific for the mycobacterial major secreted antigen 85A. *J Immunol* 165: 7088–7095.
- Wücherpfennig KW, Strominger JL (1995) Molecular mimicry in T cell-mediated autoimmunity: Viral peptides activate human T cell clones specific for myelin basic protein. *Cell* 80: 695–705.
- Zhao ZS, Granucci F, Yeh L, Schaffer PA, Cantor H (1998) Molecular mimicry by herpes simplex virus-type 1: Autoimmune disease after viral infection. *Science* 279: 1344–1347.